ON EQUILIBRIUM SOLUTIONS TO NONLOCAL MECHANISTIC MODELS IN ECOLOGY

Erin Ellefsen^{1,†}, Nancy Rodríguez¹

Abstract Understanding the factors that drive species to move and develop territorial patterns is at the heart of spatial ecology. In many cases, mechanistic models, where the movement of species is based on local information, have been proposed to study such territorial patterns. In this work, we introduce a nonlocal system of reaction-advection-diffusion equations that incorporate the use of nonlocal information to influence the movement of species. One benefit of this model is that groups are able to maintain coherence without having a home-center. As incorporating nonlocal mechanisms comes with analytical and computational costs, we explore the potential of using long-wave approximations of the nonlocal model to determine if they are suitable alternatives that are more computationally efficient. We use the gradient flow-structure of the both local and nonlocal models to compute the equilibrium solutions of the mechanistic models via energy minimizers. Generally, the minimizers of the local models match the minimizers of the nonlocal model reasonably well, but in some cases, the differences in segregation strength between groups is highlighted. In some cases, as we scale the number of groups, we observe an increased savings in computational time when using the local model versus the nonlocal counterpart.

Keywords Partial integrodifferential equations, Population dynamics, Energy, Minimizer

MSC(2010) 35Q92, 74G65.

1. Introduction

Understanding how individuals interact with each other and their environment, a core objective of theoretical ecology, is particularly crucial as climate change is altering the habitats of many species [9,19]. A recent study in Nature [13] brought forward significant evidence that 279 species (out of 1700 in their study) had been affected by climate change, and the use of mathematical models to obtain insight into this issue can be extremely powerful. In fact, local reaction-advection-diffusion (RAD) systems have been used with some success to understand territory use of various species such as coyote [10], wolves from northeastern Minnesota [21], and meerkats [1]. Such verified models can then be of use to help predict how territories

 $^{^\}dagger {\rm the~corresponding~author}.$ Email address:erin.ellefsen@colorado.edu

¹Department of Applied Mathematics, University of Colorado Boulder, Engineering Center, ECOT 225, 80309, United States

^{*}The authors were supported by NSF DMS-1516778

will evolve as the environment changes or how different groups will redistribute if a group becomes extinct.

Local RAD mechanistic models attempt to capture the social and environmental dynamics that govern how competing subgroups of a species interact with one another. Generally, local RAD models incorporate inter- and intra-group dynamics and preferences toward favorable patches in the environment [6,17]. However, there are cases where local RAD models alone are insufficient to explain certain observed phenomena without the introduction of artificial dynamics. For example, in the system introduced to model the dynamics of territory use of meerkats, an advective term pointing in the direction of an artificial home center was introduced in order to keep different groups "coherent" (by coherence we mean the non-transient formation of spatially non-constant distributions) [1]. However, recent evidence shows that some animals avoid locations where they have previously encountered a member of another group (see for example [1,5]). This implies that animals inform their decision of where to move based on nonlocal information. In fact, these nonlocal interactions can play a key role in maintaining coherence of groups. As far as we are aware, the only other work that has tried to incorporate this spatial memory is [14].

This paper has three main objectives. First, we introduce a nonlocal RAD system for multiple-species, which we argue is better suited to help maintain coherence of animal territories when there is no home center. We are concerned with studying the equilibrium solutions of this model, with particular interest in those where the territories are segregated, as this is observed in many species. We take advantage of the fact that this mechanistic model can be seen as a gradient flow of an energy (with respect to the Wasserstein metric, [20]), thus minimizers of the energy are equilibrium solutions of the mechanistic model.

This paper will thus focus on the study of the nonlocal energy that contains convolution terms, which can be computationally expensive. In [23], the authors study a system of nonlocal PDEs modeling pattern formation in marshes. They use a local approximation to predict pattern formation in the nonlocal one-dimensional model which they explore numerically. This motivates our second objective, which is to derive local approximations of the original nonlocal model and provide a comparison of the energy landscapes. Here, we present both second and fourth-order approximations and determine that, in one-dimension, the second-order approximation does a good job matching the minimizers of the nonlocal model only in a few cases. As we will see, the fourth-order matches more widely. In two-dimensions, the fourth-order approximation is required.

Our last objective is to understand how much faster (if at all) it is to find minimizers of the local energies compared to the nonlocal energy and how these savings scale with the number of species. The latter point is of particular importance, because in the model verification stage, when comparing to data, we will have to find equilibrium solutions of many groups (e.g. 6-10 depending on the application). When our algorithm was seeded random data, we discover that the local approximations can lead to significant savings in computational time. However, with two groups, when starting data close to an energy minimizer was fed to the algorithm, the computation times were similar and in some occasions, the local approximation was slower than the original nonlocal energy. With three groups in two-dimensions, we observe an increased savings in computation time with the fourth-order approximation and random starting data. For some η values, we also see increased savings

in computation time for segregated starting data. Moreover, for some starting data, the local and nonlocal algorithms find different energy minimizers. This can be attributed to the fact that the energy landscapes are complex (indeed there are an infinite number of equilibrium solutions, [16]). Note that we are often able to find a minimizer in the local approximation that matches the nonlocal minimizer provided we seed the nonlocal equilibrium to the local approximation. Incorporating an environmental potential alleviates this issue as the set of minimizers is reduced significantly. Of course, we still have non-uniqueness since for a given minimizer, if you swap populations, we obtain another minimizer. Moreover, if the environmental potential is radially symmetric, then the minimizers are invariant under rotations. Studying this case will highlight differences in segregation strength between the local and non-local models.

The model we propose is the following:

$$\partial_t u_i = \eta \Delta A(u_i) - \nabla \cdot \left[u_i \nabla \left(\mathcal{K} * u_i - \mathcal{K} * \sum_{j=1, j \neq i}^N u_j + U(x, t) \right) \right], \qquad (1.1)$$

for $x \in \Omega \subset \mathbb{R}^d$, t > 0, where $\mathcal{K} * u(x) = \int_{\Omega} K(x-y)u(y,t)dy$. Here, u_i represents different competing groups, with i=1,2,...,N. For this study we use periodic boundary conditions. A version of (1.1) was first introduced in [15] to understand social segregation. However, it can be seen as a generalization of the aggregation-diffusion equation for a single group, which has been the object of much research – see [2,4,8] and reference within. The dynamics of each group in (1.1) are governed by the competition between three forces: local diffusion (or short-range repulsion); long range intra-group attraction; and long-range inter-group repulsion.

Social interactions and social groups are not exclusive to the human population, and certain animal populations also move and live in social groups, e.g deer, wolves, lions, and meerkats [1,21,22]. The different inter- and intra-forces which have been observed, or postulated to occur, between these social groups are the factors that we incorporate into (1.1). The function A in (1.1) represents the intragroup dispersal rate, the convolution term represents intra-group aggregation, and inter-group repulsion is governed by the potential \mathcal{K} . Note that the long-range aggregation term moves the group u_i with a nonlocal velocity $-\nabla \mathcal{K} * u_i$, which helps maintain the group coherent. Moreover, the long-range, inter-group repulsion term moves the population u_i away from other groups via the velocity field $\sum_{j=1,j\neq i}^{N} \nabla \mathcal{K} * u_j$ and serves as a segregation term.

System (1.1) can be seen as a gradient flow of the following energy (with respect to the Wasserstein metric):

$$E[u_i](t) := \int_{\Omega} \left[\eta \sum_{i=1}^{N} A(u_i) - \frac{1}{2} \sum_{i=1}^{N} (\mathcal{K} * u_i) u_i + \sum_{i,j=1, i \neq j}^{N} (\mathcal{K} * u_i) u_j + \sum_{i=1}^{N} U(x,t) u_i \right] dx.$$
(1.2)

Indeed, the first variations of the energy with respect to u_i are given by:

$$\frac{\delta E}{\delta u_i} = \eta \frac{\delta A}{\delta u_i}(u_i) - \mathcal{K} * \left(u_i - \sum_{j=1, j \neq i}^n u_j \right) + U(x, t). \tag{1.3}$$

We see that we can rewrite (1.1) as

$$\partial_t u_i = \nabla \cdot \left[u_i \nabla \left(\frac{\delta E}{\delta u_i} \right) \right], \tag{1.4}$$

and write the time derivative of the energy using (1.4) and integration by parts,

$$\frac{dE}{dt} = \int_{\Omega} \left(\sum_{i=1}^{n} \frac{\delta E}{\delta u_{i}} u_{it} \right) dx$$

$$= -\int_{\Omega} \left(\sum_{i=1}^{n} u_{i} \left| \nabla \frac{\delta E}{\delta u_{i}} \right|^{2} \right) dx. \tag{1.5}$$

One of the main motivations for this work lies in the fact that solving the evolution equation (1.1) is computationally expensive as explained in the work of Bernoff and Topaz in [3]. We recap their argument for convenience. For the two-dimensional problem, if we use quadrature, the nonlocal convolution runs in $O(n^4)$ time for an $n \times n$ grid, which can be decreased to $O(n^2 \log n)$ operations with the use of pseudospectral methods. However, solutions of (1.1) can have contact lines that develop from the degenerate diffusion (as will be illustrated in what follows – see for example Figure 2) and dealing with this then requires a finer grid, increasing the computational time.

In [3], Bernoff and Topaz considered a nonlocal biological aggregation diffusion equation and derived its local approximation (a Cahn-Hilliard type equation). Their goal was to determine if the minimizers of the energy functional stemming from the original nonlocal model did a reasonable job matching the minimizer of the energy stemming from the local approximation. We use the ideas introduced in that paper and generalize them to a system of nonlocal equations. That is, we explore the use of the energy (1.2) as a way of efficiently finding equilibrium solutions. We note a few differences between this work and that of [3]. First, we focus on studying systems, which are known to behave differently than scalar equations (indeed we see a much more complex energy landscape even with two groups). We also provide a comparison of computational costs between finding the minimizers to the nonlocal energy and the local counterparts.

To use the energy as a way to find equilibrium solutions to (1.1) we consider two possible strategies. First we focus on a specific potential, the Laplace potential, which lends itself to some useful analysis, in the context of this model. This reduces the complexity of the problem, enabling us to find explicit equilibrium solutions when two groups are interacting. In the more general case, finding equilibrium solutions reduces to solving boundary value problems with a convolution that can be solved efficiently. The second approach considers more general potentials for which we perform a long-wave approximation. As mentioned earlier, our aim is to see if the local models do a suitable job approximating the nonlocal model and if it is more efficient to find equilibrium solutions of the local models.

1.1. From interacting-particles to a population density

We begin considering n distinct groups of a species interacting with each other. For each of these groups, i = 1, ..., n, there are N_i individuals and $x_k^{N_i}(t)$ denotes the

position of the k^{th} member of group i at time t. We can describe the change in position of the individual as follows:

$$\frac{dx_k^{N_i}(t)}{dt} = v_k(x, t),$$

where the velocity is given by the various interactions. Specifically, it has the form:

$$v_k(x,t) = \sum_{j=1, j \neq k}^{N_i} \nabla V(x_k^{N_i}(t) - x_j^{N_i}(t)) + \sum_{l=1}^n \sum_{j=1}^{N_l} \nabla \mathcal{K}(x_k^{N_i}(t) - x_j^{N_l}(t)) + \nabla U(x,t).$$

The potential V describes the intra-group interactions, long-range attraction and short range repulsion, \mathcal{K} describes the inter-group interactions, a weak long range force, and U describes the favorability of the environment. If we take the limit as the members of each group go to infinity, one has to consider how these interactions will change with different numbers of particles in the system. The typical scalings considered are:

$$V_N(x) = N^{\gamma_v} V_1(N^{\gamma_v/d}(x))$$
 and $\mathcal{K}_N(x) = N^{\gamma_k} \mathcal{K}_1(N^{\gamma_k/d}(x)).$

Where $\gamma_i \in (0,1)$ leads to the range of interaction decreased and the strength increased, and $\gamma_i = 0$ leads to long-range but weak interactions. Therefore, in order to match the forces we want in our model, we choose $\gamma_v \in (0,1)$ and $\gamma_k = 0$ [11,12].

In the continuum limit we arrive at the following nonlocal model for each group u and v. The diffusion term, $A(u) = u^2$ in (1.1).

$$\partial_t u_i = \eta \Delta u_i^2 - \nabla \cdot \left[u_i \nabla \left(\mathcal{K} * \left(u_i - \sum_{j=1, j \neq i}^n u_j \right) + U(x, t) \right) \right]. \tag{1.6}$$

Outline: In section 2 we derive the second and fourth-order approximations to equation (1.1) and its energy (1.2). Section 3 is devoted to the derivation of explicit equilibrium solutions to (1.1) for the Laplace potential for a two-group system and the numerical computation of the equilibrium solution for the system with three or more groups. The numerical approximation of equilibrium solutions for more general potentials is done in section 4, and we finish with a discussion in section 5.

2. Second and fourth-order approximations

In this section we derive and analyze the second and fourth-order local approximation to (1.1). Note that for two groups, constants $u_1 = u_2 = c$ are equilibrium solutions to (1.1), when $U \equiv 0$. For three groups or more, the non-local problem has only the trivial solution as a spatially homogeneous solutions. However, for the local counterparts, all constants are equilibrium solutions when $U \equiv 0$. Through linear stability analysis of these constant equilibrium solutions, we find that both approximations lead to some parameter regimes of stability. The main objective of this stability analysis is not to determine if there are parameter regimes where one expects non-constant equilibrium solutions, but rather to make sure that the approximations are not ill-posed.

The second and fourth-order approximation of the system for groups i=1,...,n is given by:

$$\partial_t u_i = \nabla \cdot \left[u_i \nabla \left(\omega u_i + \sum_{j=1, j \neq i}^n u_j + U(x, t) \right) \right]. \tag{2.1}$$

and

$$\partial_t u_i = \nabla \cdot \left[u_i \nabla \left(\omega u_i - \nabla^2 u_i + \sum_{j=1, j \neq i}^n (u_j + \nabla^2 u_j) + U(x, t) \right) \right], \qquad (2.2)$$

respectively, with $\omega = 2\eta - 1$. Both approximations enjoy a gradient-flow structure with the following the respective energies:

$$E_{L2}[u_1, ..., u_n] := \int \left(\frac{\omega}{2} \sum_{i=1}^n u_i + \sum_{i,j,i \neq j}^n u_i u_j + \sum_{i=1}^n U(x,t) u_i\right) dx$$
 (2.3)

$$E_{L}[u_{1},...,u_{n}] := \int \left(\frac{\omega}{2} \sum_{i=1}^{n} u_{i}^{2} + \frac{1}{2} \sum_{i=1}^{n} |\nabla u_{i}^{2}| - \sum_{i,j,i\neq j} (\nabla u_{i} \cdot \nabla u_{j} - u_{i}u_{j}) + \sum_{i=1}^{n} U(x,t)u_{i}\right) dx.$$

$$(2.4)$$

In the remainder of the paper we work with interacting potentials K that satisfy the following assumptions:

- 1. \mathcal{K} is radial: $\mathcal{K}(x) = \mathcal{K}(|x|)$;
- 2. $\mathcal{K} \in L^1(\mathbb{R}^d)$ with unit mass: $\int_{\mathbb{R}^d} \mathcal{K}(y) dy = 1$;
- 3. K has sufficient decay as $|x| \to \infty$: defining

$$M_m := \frac{1}{m!} \int_{\mathbb{R}^d} \mathcal{K}(z) z^m dz;$$

we assume that $\lim_{m\to\infty} M_m = 0$ and $M_{m+1} = o(M_m)$;

4. K has a normalized second moment $M_2 = 2d$.

2.1. Long-wave approximations

To obtain a local approximation to the nonlocal model, we perform long-wave approximation of the nonlocal term under the assumption for the interaction potential discussed above, exactly as found in [3], but details are included for the reader's convenience. The main thing to consider is that we can approximate the convolution term by first taking the Fourier Transform of the potential and keeping the long-wave modes. By assumption, \mathcal{K} is radial and thus its Fourier Transform is also radial in k. We have

$$\hat{\mathcal{K}}(k) = \int_{\mathbb{R}^n} \mathcal{K}(r)e^{-i\mathbf{k}\mathbf{x}}d\mathbf{x},$$

where $k = |\mathbf{k}|$ and $r = |\mathbf{x}|$. We rewrite the exponential in series form,

$$e^{-i\mathbf{k}\mathbf{x}} = \sum_{m=0}^{\infty} (-i)^m \frac{\mathbf{k} \cdot \mathbf{x}}{m!};$$

and obtain that:

$$\hat{\mathcal{K}}(k) = \int_{\mathbb{R}^d} \left(\mathcal{K}(r) - \mathcal{K}(r) i \mathbf{k} \cdot \mathbf{x} - \frac{1}{2} \mathcal{K}(r) (\mathbf{k} \cdot \mathbf{x})^2 + \cdots \right) d\mathbf{x}.$$

Using the assumptions on \mathcal{K} , we find the second and forth terms to be zero due to symmetry, and the first term, $\int_{\mathbb{R}^d} \mathcal{K}(z)dz = 1$. For the third term, we have

$$-\frac{1}{2} \int_{\mathbb{R}^d} (\mathbf{k} \cdot \mathbf{x})^2 K(r) d\mathbf{x} = -\frac{1}{2} \sum_{p=1}^d \sum_{q=1}^d k_p k_q \left[\int_{\mathbb{R}^d} \mathcal{K}(r) x_p x_q d\mathbf{x} \right]$$
(2.5)

$$= -\frac{1}{2} \sum_{p=1}^{d} k_p^2 \left[\int_{\mathbb{R}^d} \mathcal{K}(r) x_p^2 d\mathbf{x} \right]$$
 (2.6)

$$= -\frac{1}{2} \sum_{p=1}^{d} k_p^2 \left[\frac{1}{d} \int_{\mathbb{R}^d} \mathcal{K}(r) r^2 d\mathbf{x} \right]$$
 (2.7)

$$= -\frac{1}{2} \frac{1}{d} 2d \sum_{p=1}^{d} k_p^2$$

$$= -k^2.$$
(2.8)

We rewrite $(\mathbf{k} \cdot \mathbf{x})^2$ as a double sum in the right hand side of (2.5), (2.6) uses symmetry to conclude that the non-diagonal terms cancel, (2.7) uses the radial symmetry of \mathcal{K} to arrive at the second moment, and (2.8) substitutes in the assumption we have made for M_2 . Finally, using the first three terms in the approximation, we get $\hat{\mathcal{K}} = 1 - k^2 + O(k^4)$. From this, we obtain second-order approximation by taking $\mathcal{K} * w \approx w$ and substituting this back into (1.6) to get (2.1). On the other hand, substituting $\mathcal{K} * w \approx w + \nabla^2 w$ gives the fourth-order approximation seen in (2.2).

2.2. Stability analysis for the local approximations

To determine the viability of using these local approximations, we start by performing a stability analysis for both approximations when the number of groups interacting with each other is two or three. We find parameter regimes leading to stability for both approximations; however, as expected, the fourth-order approximation has a larger regime of stability. Of course, this comes at the cost of having more terms to deal with analytically and numerically. Thus, for the purpose of fast computations ideally one would prefer to work with a second-order approximation.

Proposition 2.1. We obtain the following conditions to achieve linear stability for the local approximations, (2.1) and (2.2):

- 1. The second-order approximation, (2.1), with U=0, achieves linear stability for n=2 and n=3 when $\eta>1$.
- 2. The fourth-order approximation, (2.2), with U = 0, achieves linear stability for n = 2 when $\eta > 1/2$.
- 3. The local approximations, (2.1) and (2.2), with $U \neq 0$ achieve linear stability for n = 2 when $\Delta U < 0$.

The proof of this proposition relies on lemmas which we state and prove below.

2.3. Second-order approximation with no environment

We begin with the stability analysis of (2.1) for n = 2 and n = 3 with the following result:

Lemma 2.1. Let U = 0. Then, (2.1) achieves linear stability for n = 2 and n = 3 when $\eta > 1$.

Proof. Consider perturbations of the form $u = \bar{u} + \delta_u e^{ikx+\sigma t}$ and $v = \bar{v} + \delta_v e^{ikx+\sigma t}$. The resulting linear system is:

$$\sigma \begin{bmatrix} \delta_u \\ \delta_v \end{bmatrix} = \begin{bmatrix} -\omega \bar{u}k^2 & -\bar{u}k^2 \\ -\bar{v}k^2 & -\omega \bar{v}k^2 \end{bmatrix} \begin{bmatrix} \delta_u \\ \delta_v \end{bmatrix}.$$

Note that the determinant of the matrix is $D = (\omega^2 - 1)\bar{u}\bar{v}k^4$ and it is positive when $\omega^2 - 1 > 0$ which corresponds to $\eta > 1$. The trace, $T = -\omega k^2(\bar{u} + \bar{v})$, is negative when $\omega > 0$, corresponding to $\eta > 1/2$. Therefore, for (2.1), we get linear stability for $\eta > 1$.

When n=3, we substitute the perturbation of the constant solution, $w=\bar{w}+\delta_w e^{ikx+\sigma t}$ and linearize the system in the same manner. The resulting system is given by:

$$\sigma \begin{bmatrix} \delta_u \\ \delta_v \end{bmatrix} = \begin{bmatrix} -\omega \bar{u}k^2 & -\bar{u}k^2 & -\bar{u}k^2 \\ -\bar{v}k^2 & -\omega \bar{v}k^2 & -\bar{v}k^2 \\ -\bar{w}k^2 & -\bar{w}k^2 & -\omega \bar{w}k^2 \end{bmatrix} \begin{bmatrix} \delta_u \\ \delta_v \\ \delta_w \end{bmatrix}.$$

Here we can use the Routh-Hurwitz criterion, [18], to determine when the the eigenvalues are in the left half of the complex plane. We first find the characteristic equation,

$$p(\lambda) = -\lambda^3 - \omega k^2 (\bar{u} + \bar{v} + \bar{w}) \lambda^2 + k^4 (\bar{v}\bar{w} + \bar{u}\bar{w} + \bar{u}\bar{v}) (1 - \omega^2) \lambda + k^6 \bar{u}\bar{v}\bar{w} (-2 + 3\omega - \omega^3).$$

From the characteristic equation, we obtain:

$$a_0 = k^6 (\bar{u}\bar{v}\bar{w})(2 - 3\omega + \omega^3)$$

$$a_1 = -k^4 (\bar{v}\bar{w} + \bar{u}\bar{w} + \bar{u}\bar{v})(1 - \omega^2)$$

$$a_2 = \omega k^2 (\bar{u} + \bar{v} + \bar{w}).$$

We have linear stability when $a_0 > 0, a_2 > 0$, and $a_2a_1 > a_0$. We first consider when $a_2a_1 - a_0$ is greater than zero:

$$a_2a_1 - a_0 = 2k^6\bar{u}\bar{v}\bar{w}(\omega^3 - 1) + k^6(\bar{u}^2(\bar{w} + \bar{v}) + \bar{v}^2(\bar{w} + \bar{u}) + \bar{w}^2(\bar{u} + \bar{v}))(\omega^3 - \omega).$$

We see the coefficients of $\omega^3 - 1$ and $\omega^3 - \omega$ are positive. We also have $\omega^3 - \omega$ and $\omega^3 - 1$ are positive when $\omega > 1$. This corresponds to $\eta > 1$. It is quick to check that $a_0, a_2 > 0$ when $\eta > 1$ as well. Therefore, the system is linearly stable for $\eta > 1$.

Note that we can use the Routh-Hurwitz criterion for higher dimensional systems in order to determine stability for an artibrary number of groups.

2.4. Fourth-order approximation with no environment

Lemma 2.2. Let U = 0 and n = 2. The fourth order approximation, (2.2), achieves linear stability when $\eta > 1/2$.

Proof. For the fourth-order approximation, the corresponding linear system with two groups is:

$$\sigma \begin{bmatrix} \delta_u \\ \delta_v \end{bmatrix} = \begin{bmatrix} -k^2(\omega + k^2)\bar{u} & k^2(k^2 - 1)\bar{u} \\ k^2(k^2 - 1)\bar{v} & -k^2(\omega + k^2)\bar{v} \end{bmatrix} \begin{bmatrix} \delta_u \\ \delta_v \end{bmatrix}.$$

The determinant $D = k^4 \bar{u}\bar{v}[(\omega + k^2)^2 - (k^2 - 1)^2]$ is positive if

$$(\omega + k^2)^2 > (k^2 - 1)^2$$
, or $(2\eta - 1 + k^2)^2 > (k^2 - 1)^2$.

This is true if $\eta > 0$. For the trace, $T = -k^2(\bar{u} + \bar{v})(\omega + k^2)$, to be negative we need $\omega + k^2 > 0$, or $1 - 2\eta < k^2$. If $\eta > 1/2$, $1 - 2\eta$ is always negative, so it is less than k^2 . For $\eta > 1/2$, we get linear stability.

Therefore, we see that the fourth-order approximation is stable for a larger region of η than the second-order approximation.

2.5. Stability with an environment term

For simplicity, we only consider the case with two interacting groups when adding an environmental potential U to our system.

Lemma 2.3. Let n=2 and $U \neq 0$. The local approximations, (2.1) and (2.2), achieve linear stability when $\Delta U < 0$.

Proof. The equilibrium solutions are now $\bar{u}=0$ and $\bar{v}=0$. So, our perturbations are now simply $u=\delta_u e^{ikx+\sigma t}$ and $v=\delta_v e^{ikx+\sigma t}$. Substituting those into the system and keeping only linear terms in δ_u, δ_v both in the second and fourth-order approximations gives us the resulting system:

$$\sigma \begin{bmatrix} \delta_u \\ \delta_v \end{bmatrix} = \begin{bmatrix} ik\nabla U(x,t) + \Delta U(x,t) & 0 \\ 0 & ik\nabla U(x,t) + \Delta U(x,t) \end{bmatrix} \begin{bmatrix} \delta_u \\ \delta_v \end{bmatrix}.$$

With an environment potential, the only constant equilibrium solution is the trivial. Therefore, we obtain a simple diagonal matrix when we perturb them and keep linear terms. The eigenvalues are the diagonal entries. In order to have real part negative, we must have $\Delta U(x,t) < 0$. Therefore, we need the environment potential to be concave down for stability.

Now we are ready to prove Proposition 2.1.

Proof. (Proposition 2.1)

Combined, Lemma 2.1, Lemma 2.2, and Lemma 2.3 prove our result. □

3. Equilibrium solutions for the Laplace potential

Strategically choosing certain potentials can help streamline the analysis of the system. To illustrate this, in this section we consider the Laplace potential, which is the Green's function of the Helmholtz equation. A nice consequence of this is that for two groups we obtain analytical equilibrium solutions to (1.1). This is not the case for n groups, but we do obtain a reduced model, a nonlocal boundary-value problem where the nonlocal term is the convolution. Recall that the Laplace potential, $\mathcal{K}(x) = \frac{1}{2m} e^{-m|x|}$, satisfies:

$$\mathcal{K}_{xx} - m^2 \mathcal{K} = -\delta(x). \tag{3.1}$$

3.1. Two groups: n = 2

We consider two groups, denoted by u and v. Using the gradient-flow structure observed in (1.5), we can substitute (1.3) for both groups u and v and analyze the equilibrium solutions to obtain:

$$0 = -\int_{\mathbb{R}^d} \left(u \left| \nabla \frac{\delta E}{\delta u} \right|^2 + v \left| \nabla \frac{\delta E}{\delta v} \right|^2 \right) dx$$
$$= -\int_{\mathbb{R}^d} \left(u \left| \nabla (2\eta u - \mathcal{K} * (u - v)) \right|^2 + v \left| \nabla (2\eta v - \mathcal{K} * (v - u)) \right|^2 \right) dx.$$

Note that $u, v \ge 0$ are physical constraints on the solution we care about and thus the integrand above must be non-negative. This enforces that the integrand be zero, meaning that both terms in the integrand must vanish. Thus,

$$0 = u |\nabla (2\eta u - \mathcal{K} * (u - v))|^2 = v |\nabla (2\eta v - \mathcal{K} * (v - u))|^2.$$

From here, we deduce that $\nabla(2\eta u - \mathcal{K}*(u-v)) = \nabla(2\eta v - \mathcal{K}*(v-u)) = 0$, implying that:

$$2\eta u - \mathcal{K} * (u - v) = c_1 \tag{3.2}$$

$$2\eta v - \mathcal{K} * (v - u) = c_2 \tag{3.3}$$

where c_1, c_2 are constants. Solving for u + v gives:

$$u + v = \frac{c_1 + c_2}{2\eta}. (3.4)$$

Now hitting (3.2) with the operator $\partial_{xx} - m^2$ and recalling that \mathcal{K} satisfies (3.1) allows us to compute as follows:

$$2\eta(u_{xx} - m^2u) - \int_{\mathbb{R}} (\partial_{xx} - m^2) \mathcal{K}(x - y) (u(y) - v(y)) dy = -m^2 c_1$$

$$2\eta(u_{xx} - m^2u) + u(x) - v(x) = -m^2 c_1$$

$$2\eta(u_{xx} - m^2u) + u(x) - \frac{c_1 + c_2}{2\eta} + u = -m^2 c_1$$

$$u_{xx} + (1/\eta - m^2)u = \frac{(1 - 2\eta m^2)c_1 + c_2}{4\eta^2}$$
(3.5)

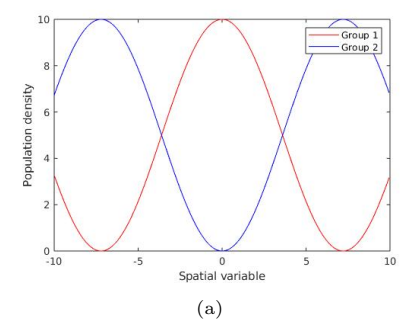
In the case when $\eta m^2 < 1$, we can solve this second-order differential equation explicitly.

$$u(x) = A\cos(\sqrt{1/\eta - m^2}x) + B\sin(\sqrt{1/\eta - m^2}x) + \frac{(1 - 2\eta m^2)c_1 + c_2}{4\eta^2(1/\eta - m^2)}$$

Using the relation in (3.4), we can explicitly write v,

$$v(x) = \frac{c_1 + c_2}{2\eta} - A\cos(\sqrt{1/\eta - m^2}x) - B\sin(\sqrt{1/\eta - m^2}x) + \frac{(1 - 2\eta m^2)c_1 + c_2}{4\eta^2(1/\eta - m^2)}.$$

One of these analytical solutions is illustrated in Figure 1(a). We can consider how the restriction $\eta m^2 < 1$ can be interpreted physically. Decreasing m leads to a steeper segregation potential, and increasing the parameter η increases the diffusion of the groups. Therefore, as we increase the steepness of the potential, we can allow for larger diffusion, or a group with smaller density. This suggests that if groups have a stronger repulsion from each other, they can take up more space. As we decrease the steepness of the potential, we must have smaller diffusion, or higher mass for the group. Thus, if the groups are not as strongly repulsed from each other, they must take up less space. This interplay between these parameters suggests a balance that leads to the territory segregation we see in Figure 1(a).



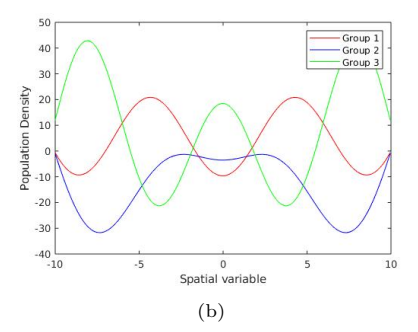


Figure 1. (a) Analytical solution to (3.5) with two groups interacting (b) The least squares solution to the linear system (3.7) with three groups.

3.2. General number of groups: n > 2

The nice cancellations that occurred in the above section do not happen in the more general case; however, we can still follow the procedure discussed above to reduce the system's complexity. Indeed, we obtain a system of ODEs that we can solve recursively for group i = 1, ..., n. We can use the symmetry of the system to get the remaining ODEs. An appropriate linear combination of (1.3), gives the following:

$$\sum_{i=2}^{n} u_i = (n-3)u_1 - \frac{n-2}{\eta}K * u_1 - \frac{n-3}{2\eta}c_1 + \frac{1}{2\eta}\sum_{i=2}^{n} c_i$$
 (3.6)

If we hit (1.3) for i = 1 with the operator $\partial_{xx} - m^2$ and substitute in (3.6), we have the resulting ODE:

$$u_{1xx} - \left(m^2 + \frac{n-4}{2\eta}\right)u_1 + \frac{n-2}{2\eta^2}K * u_1 = \frac{(-2\eta m^2 - n + 3)c_1 + \sum_{i=2}^n c_i}{4\eta^2}.$$
 (3.7)

The obvious algorithm to use for solving this ODE is the Fast Fourier Transform (FFT), [7]. Taking the Fourier Transform of (3.7) and solving for \hat{u}_1 gives that:

$$\hat{u}_1(w) = \frac{(2\eta m^2 - n + 3)c_1 + \sum_{i=2}^n c_i}{4\eta^2 \left(-w^2 - \left(m^2 + \frac{n-4}{2\eta}\right) + \frac{n-2}{2\eta^2 (1+w^2)}\right)} \delta(\omega). \tag{3.8}$$

Therefore, in order to find u_1 and therefore u_i by symmetry, we need to find the inverse Fourier Transform of (3.8). Note that this returns the constant solution of the ODE. Recall that the boundary value problem is not unique. In fact, we get this same result using this method on the ODE obtained with two groups.

To obtain non-constant solutions, we discretize the domain and approximate u_{xx} with centered differences and approximate the convolution with the same matrix multiplication that we use in our numerical results in Section 4, reducing the problem to solving a linear system. Figure 1(b) illustrates a solution, while these solutions are negative in some values, the overall solution provides the territory boundaries when three groups are interacting in a one-dimensional space. In this case, we could interpret territory boundaries by shifting solutions above y=0.

4. Energy minimizers for general potentials

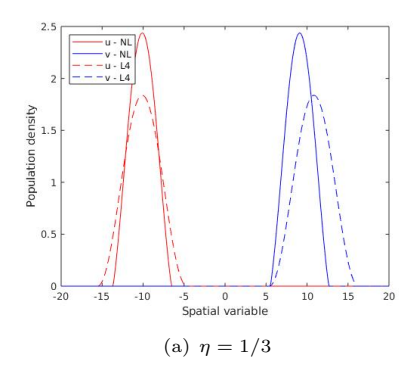
To consider more general potentials we resort to computing the energy minimizers numerically, which we do through the use of fmincon from MatLab's optimization toolbox, computing the convolution via matrix multiplication using a equispaced grid, and computing derivatives using centered differences. We use the Laplace potential for each case, normalized to satisfy the assumptions put on our potential, $K(x) = -a_1 e^{a_2|x|}$, where $a_1 = \frac{\pi}{\Gamma(\frac{d+1}{8\pi})} \left(\frac{d+1}{8\pi}\right)^{d/2}$, $a_2 = \sqrt{\frac{d+1}{2}}$.

4.1. One-dimensional energy minimizers

For proof of concept we begin with the one-dimensional case. Our analysis begins with considering the interaction between two groups and we compare the local and nonlocal minimizers of their respective energies. Additionally, we contrast the computational time required for the algorithm to find the minimizers when seeded (1) random starting data and (2) segregated starting data (i.e. presumably close to what we believe to be a minimizer). The scaling of these computational times as we add more groups is very important for real world applications; hence, we also study what happens when we have three groups interacting. The final case we analyze in one-dimension is the addition of an environment potential.

4.1.1. Two groups interacting with no environmental influence

First, consider the case of two groups interacting with no environmental influence. From our analysis, for random starting data, we observe that the fourth-order local model is a better approximation to the nonlocal model in comparison to the second-order model. The second-order approximation either does not match the nonlocal model or is unstable, by which we mean that the algorithm did not return a reasonable minimizer. The latter was the case for the numerical experiments illustrated in Figure 2, which is the reason that results from the second-order approximation are not included. The results illustrated in Figure 2 are as expected:



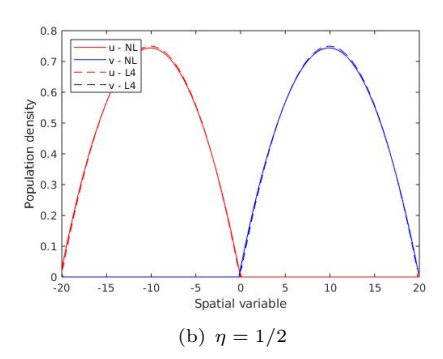
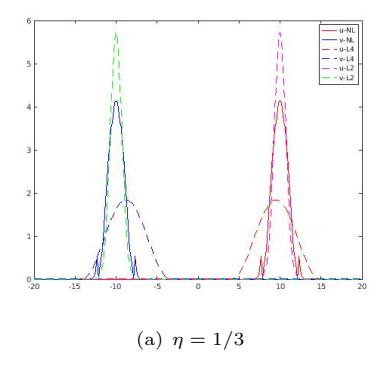


Figure 2. Energy minimizers for random starting data. NL refers to the non-local model and L4 to the 4th-order approximation.



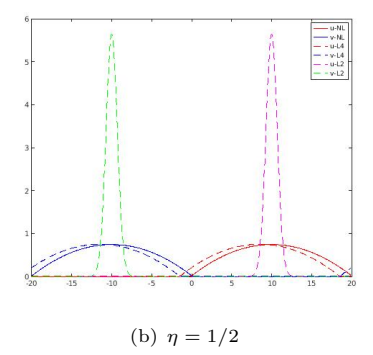


Figure 3. Energy minimizers for segregated starting data. NL refers to the non-local model, L2 and L4 to the 2nd-order and 4th-order approximations, respectively.

the two groups form territories that are segregated, but have larger territories as η increases. For lower values of η , the minimizers for the fourth-order local energy tend to be shorter and wider than the minimizers for the nonlocal energy. Also note that as η increases, the fourth-order approximation does a better job matching the nonlocal equilibrium. A potential reason for this behavior is the desire to segregate is stronger in the nonlocal model than in the local counterpart. We observe that this difference diminishes as the two groups diffuse more and thus have less space to occupy (due to the boundedness of the domain), see Figure 2.

When seeding the minimizer algorithm segregated data, we often find minimizers of higher energy as compared to the minimizers obtained when seeding the algorithm random data. Recall that these energies are not convex and there are many local minimizers, which our algorithm will find depending on the data seeded. In fact, in all of our simulations, we found a minimizer of higher or equal energy when we seeded segregated data versus random data. This implies that we are more likely to get to a global minimizer if seeding the algorithms random data. Comparing the nonlocal minimizers illustrated in Figures 2(a) and 3(a), we note that the former has lower energy than the latter. Also, the nonlocal minimizers illustrated in 2(b) and

η	1/6	1/3	1/2	2/3	5/6
Nonlocal	78	153	78	33	23
Local-4th order	56	40	67	75	102

Table 1. Computational time in seconds for two groups interacting with no environmental influence and with a random starting data.

3(b) have equal energy. In Figure 3, the minimizer of the nonlocal model is not a minimizer of the fourth-order approximation, but is a minimizer of the second-order approximation. Hence, there are rare cases where the second-order approximation matches the nonlocal and the fourth-order approximation does not.

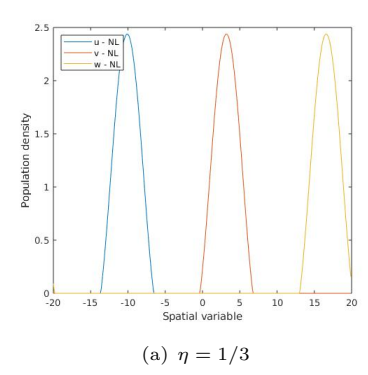
We must also point out that in some cases, when the algorithm was fed segregated data, the minimizer of the fourth-order approximation did not match the nonlocal minimizer. However, this was never the case when seeded random data. The second-order approximation matched in rare cases, but was unstable more often than not. For these reasons, we find the fourth-order approximation to be more suitable.

When comparing computational time, the fourth-order approximation performed at about the same level as the nonlocal counterpart, this is illustrated in Table 1. Thus, while the fourth-order approximation seems to be a suitable replacement for the nonlocal model, it does not save computational time in one-dimension. Interestingly, for smaller values of η the local approximation was faster, but for larger values of η computing the minimizer for the nonlocal energy was faster. The computational times for segregated starting data are not shown in Table 1, because when feeding the algorithm a starting point close to an energy minimizer it takes at most two seconds for any of the models to find the minimizer. If the data seeded to the algorithm is not close to a minimizer, the results are similar to those with random starting points. In either case the fourth-order approximation does not really save computational time in the one-dimensional case with two-species interacting.

4.1.2. Three groups interacting with no environmental influence

η	1/6	1/3	1/2	2/3	5/6
Nonlocal - 2 Groups	78	153	78	33	23
Nonlocal - 3 Groups	563	1460	268	143	138

Table 2. Computation times in seconds for three groups with no environmental influence and random starting data.



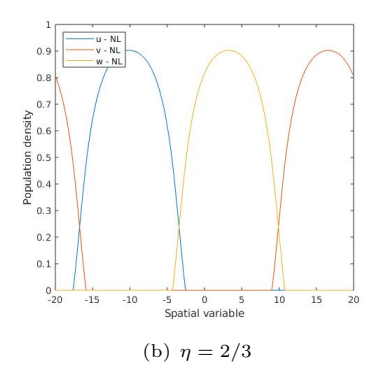
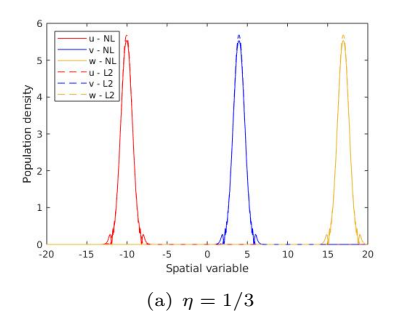


Figure 4. Minimizers for random starting data for the nonlocal model with different η values.



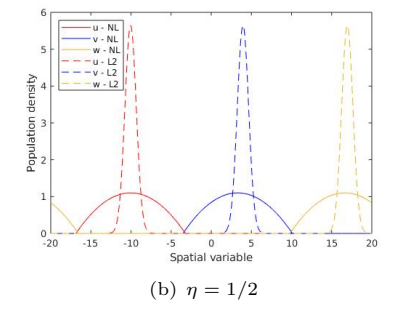


Figure 5. Minimizers for segregated starting data

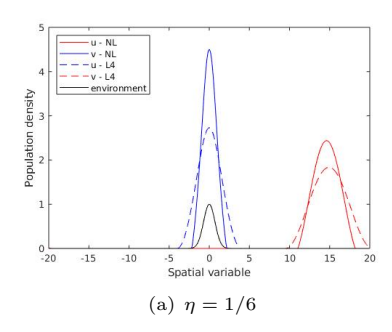
Next, we look at energy minimizers when three groups interact with no environmental influence. When considering random starting data, in contrast to the previous case studied, both the fourth-order and the second-order approximation returned unstable results. Therefore, we only illustrate the nonlocal minimizers in Figure 4, where we observe intuitive results as we did with two groups.

For segregated starting data, the results for the nonlocal model and the second-order approximation are very similar to the previous case. The fourth-order approximation remains unstable. We see matches between the nonlocal and the second-order approximation in some cases, for example, for $\eta=1/3$, as illustrated in Figure 5(a). In contrast, for $\eta=2/3$, the starting data remains near a steady state for the second-order approximation, and is no longer a steady state for the nonlocal model. Therefore, the second-order approximation does not appear match the nonlocal model for the data seeded as η increases. Moreover, as in earlier cases, the energies of the minimizers found with random starting data are lower than or equal to the energies found with segregated starting data.

We also analyze the computational expense incurred when adding a group to the nonlocal model. These times are displayed in Table 2. Adding a group significantly increases computational time, as we can see from the time differences shown in Table 2. The computational time for segregated starting data is not included, for

the same reasoning as previously mentioned.

4.1.3. Two groups interacting with an environmental influence



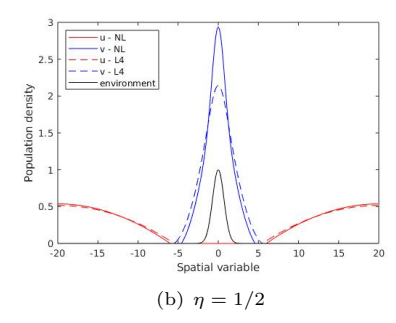


Figure 6. Minimizers of the nonlocal and the fourth-order approximation energy for random starting data.

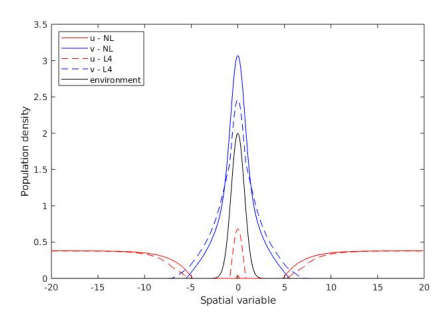


Figure 7. Minimizers of the nonlocal and fourth-order approximation energies with random starting data, $\eta = 2/3$, a = 2.

Finally, we investigate the effect of an environmental potential which influences the movement of all groups. With random starting data, as expected for the nonlocal model, if the influence of the environmental potential is strong enough, it overpowers the desire for groups to segregate. However, there is some balance found between establishing a territory where groups see environmental benefits while being reasonably segregated. This balance is illustrated in Figure 6, where we have used the environmental potential $U = ae^{-x^2}$ with a = 1. the change of the environmental strength is done by changing the value of a.

For weak diffusion coefficients, as seen in Figure 6(a), one group tends to overpower regions that provide a good environment. The group that dominates depends on the seeded data (i.e. it is random if the seeded data is random). For larger values of η , the groups remain segregated but are closer and the second group is closer to the environment potential, illustrated in 6(b). Like the cases without the environment potential, the minimizers of the local energy were often shorter and wider for lower η values.

	Environment			No Environment				
η	1/6	1/3	1/2	2/3	1/6	1/3	1/2	2/3
Nonlocal	38	39	31	21	78	153	78	33
Local-4th order	51	42	53	69	56	40	67	75

Table 3. Computational times for two groups with an environment potential, random starting data

The environment potential also highlights some differences between the nonlocal model and local approximation that we have not seen previously. In Figure 7, the strength of the environment potential (a=2) overpowered the segregation in the fourth-order local approximation: both groups have some claim to territory where the environment is beneficial, and their territories overlap. However, the desire to segregate remains strong in the nonlocal minimizers. In fact, only one group has established territory in regions where the environment is good and there is no territory overlap. Moreover, without the influence of an environment potential, higher η values diminished the differences in segregation between the local and nonlocal minimizers. On the other hand, with an environment potential, we observe the stronger sense of segregation in the nonlocal model for higher η values.

For segregated starting data, we obtain similar results to those seen when we considered no environmental influence. The second-order approximation matched local minimizers in limited cases, but was often unstable, and therefore is not displayed. The energy minimizers of the fourth-order approximation provide a reasonable match for most of the minimizers found using segregated data and matched the minimizers of lowest energy found. It produced stable results for a wide range of η values.

The computational times for two groups with an environmental influence are shown in the Table 3 for random initial data. We again omit the table for segregated starting data for the same reasons as the previous cases. The times suggest that the addition of the environment potential may, on average, slightly speed up the computation for a random starting data as compared to the results for two groups without the environmental potential. These are also listed in Table 3 for comparison. However, it is still clear that in one-dimension, the fourth-order approximation did not save computation time, and in many cases, it was more computationally expensive.

4.2. Two-dimensional energy minimizers

In this section, we perform an analysis which is analogous to that done in onedimension. However, as two-dimensional domains are physical for many applications in spatial Ecology, the results from these sections are relevant from the application perspective. When investigating both the second and fourth-order approximations in two-dimensions, the results from the second-order approximation are not stable and we are forced to use the fourth-order approximation. Therefore, in this section we only analyze and compare the fourth-order local approximation to the nonlocal counterpart.

4.2.1. Two groups with no environmental influence

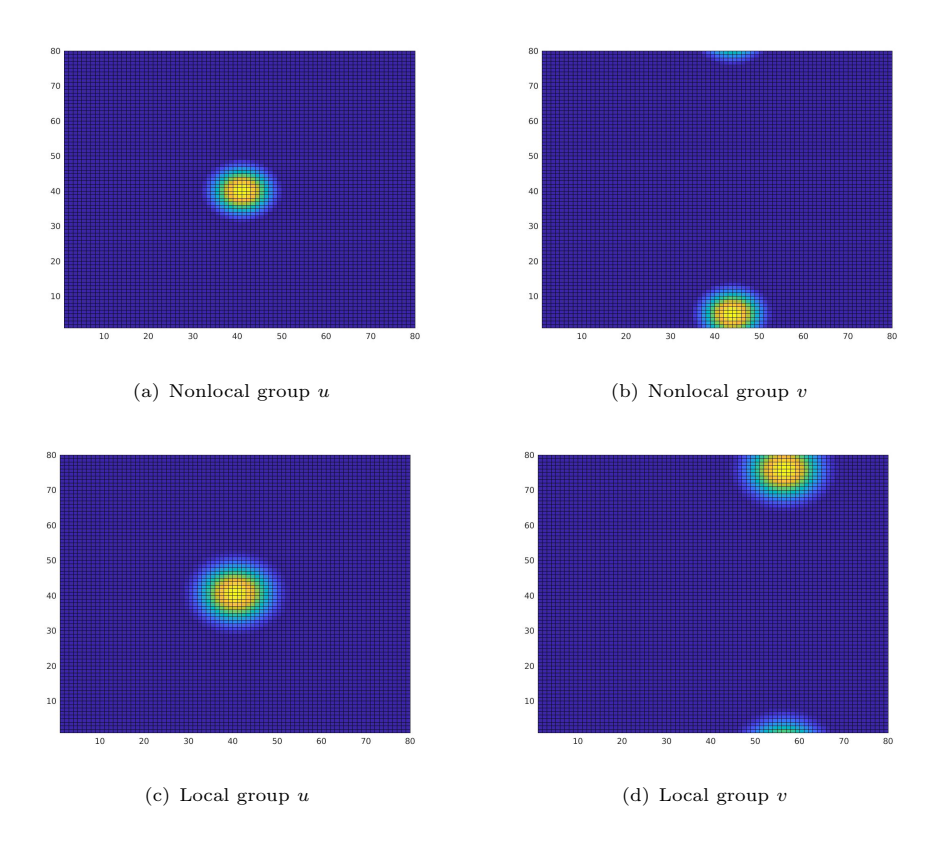


Figure 8. Energy minimizers for the local and nonlocal models with $\eta = 1/3$.

For two groups with no environmental influence, we obtain results mirroring those seen in one-dimension. For random starting data, the local model matches the nonlocal model reasonably well, as we see in Figure 8. In some cases, like Figure 8, the minimizer of the local energy is slightly translated and has a larger territory than the nonlocal minimizer. This effect diminishes as η increases, just as we saw in one dimension.

For segregated starting data, we find that in many cases, the fourth-order local approximation matches the nonlocal model well. However, in some cases the nonlocal model returns a different minimizer than the local model. Just as we saw in one dimension, the nonlocal minimizers that do not match the local approximation, in each case, have been minimizers with a higher energy than those found with random starting data.

When comparing computation time, we find differences between the one-dimensional and two-dimensional case. In two-dimensions, if the algorithm was fed random starting data, the local approximation terminated much faster than the nonlocal. This is likely because in one-dimension, we implement the convolution

	Rando	m Startin	Segregated Starting Data			
η	1/6	1/3	1/2	1/6	1/3	1/2
Nonlocal	> 600000	509988	> 600000	16	3121	767
Local	17202	45452	112098	13	24	5252

Table 4. Computational times (s) for two groups in two-dimensions.

with an $N \ge N$ matrix, but in two-dimensions, in order to implement the convolution, we use an $N^2 \ge N^2$ matrix, so the time complexity is much larger when we increase to two-dimensions. The computation time for random starting data can be found in Table 4. However, when fed starting data closer to a minimizer (i.e. segregated territories), the computation time was similar. There were cases ($\eta = 1/3$) where the local model terminated faster, but also cases when the nonlocal model terminated faster ($\eta = 1/2$). Some of these computation times are displayed in Table 4.

4.2.2. Two groups with an environment potential

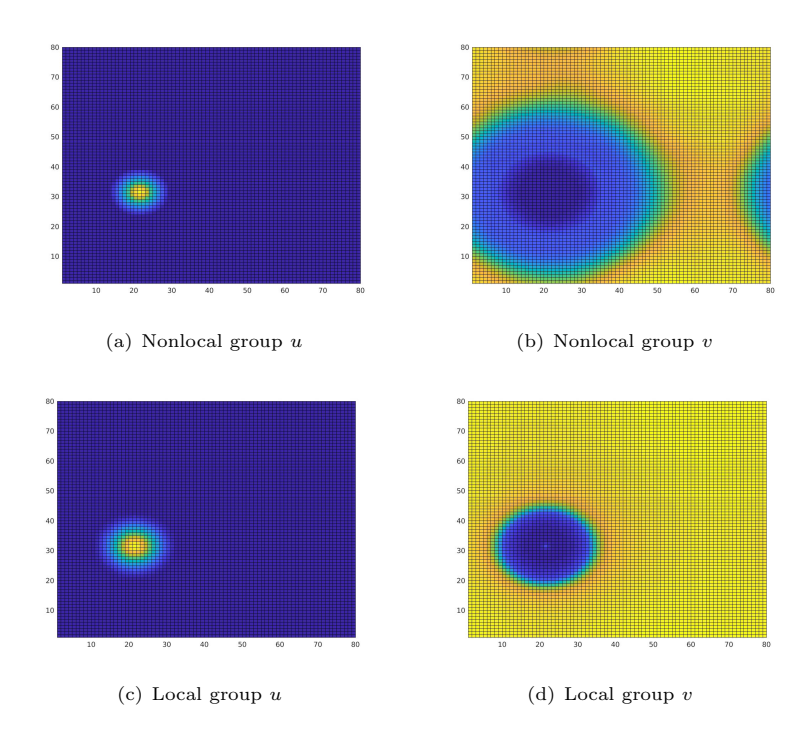


Figure 9. Energy minimizers for the local and nonlocal model with an environment potential with $\eta=1/3$

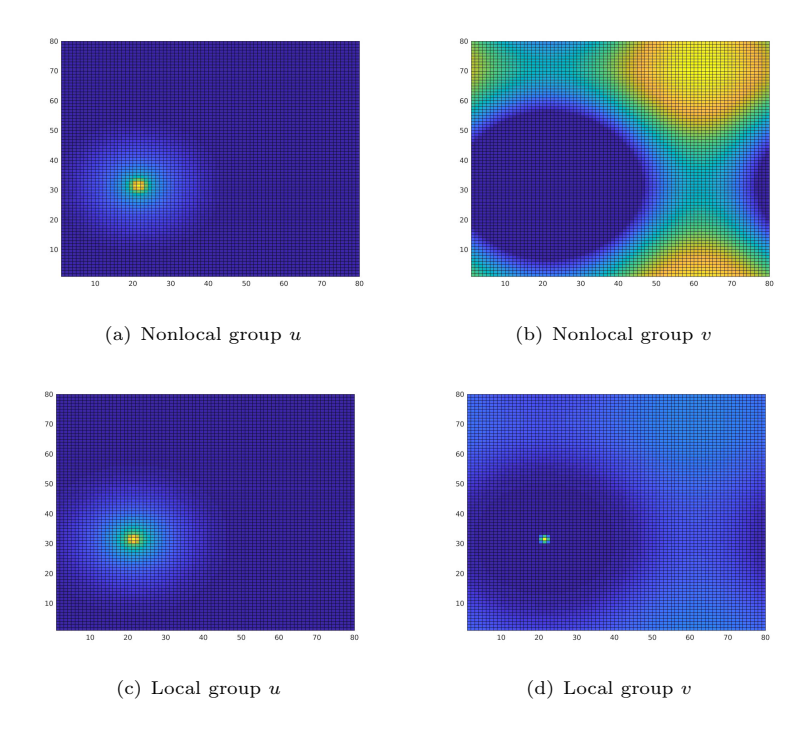


Figure 10. Energy minimizers for the nonlocal model and local approximation with an environment potential, $\eta = 1/2$

η	1/6	1/3	1/2	
Nonlocal	177161	84358	70929	
Local	16613	14242	43122	

Table 5. Computation times in seconds for two groups with an environment potential, random starting data

Here, we observe analogous results to the one-dimensional case when we include an environmental influence. Figure 9 illustrates results in two dimensions, with environmental potential $U = e^{-\frac{1}{4}((x-20)^2+(y-30)^2)}$, that can be compared to Figure 6, which illustrates results one-dimension. One group overpowers the territory where there are environmental benefits, and the other group crowds closely by while maintaining some segregation. As we have in one-dimension, the group that develops their territory with environmental benefits depends on the random starting data.

When comparing the nonlocal model and the local model, we also see results similar to those observed in one-dimension. At lower η values, we see that the nonlocal model often has higher population density, it retains more segregation than the local model. When η increases or the mass of the population increases, we see better matches if there is no environment term. However, with an environment

term, the desire to be in environmentally beneficial locations overpowers the desire to segregate in the local model: the groups develop overlapping territories over beneficial environment. On the other hand, the desire to segregate remains strong in the nonlocal model. Figure 10 displays this discrepancy. It is enlightening to see what a possible cross-section of Figure 10 might look like by referencing the analogous one dimensional figure, Figure 7.

Similar to the results in one dimension, the computation time is sped up with an environment potential, but in two-dimensions, it is considerably faster than without an environment term. This can be seen in the differences in Table 4 and 5. It is also still the case that with random starting data, the local model terminates much faster than the nonlocal model.

4.2.3. Three groups with no environmental influence

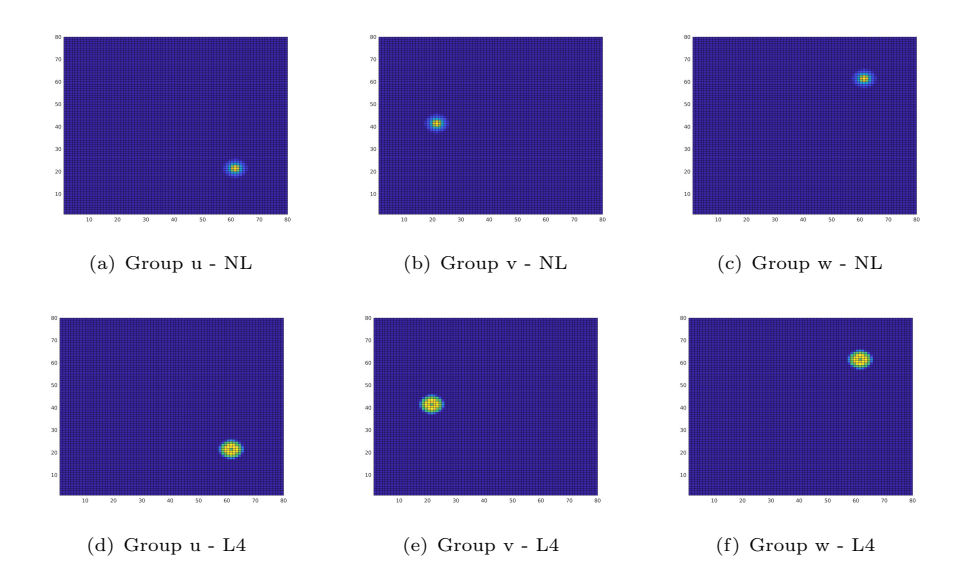


Figure 11. Energy minimizer for three groups with a segregated starting point for both the nonlocal and local model and $\eta = 1/3$.

Finally, we found energy minimizers in two-dimensions with three groups. The computational expense it took to add a group in the nonlocal model in two-dimensions with random starting data was too great for the algorithm and our resources, although we were able to get results with segregated starting data. We found interesting results when comparing to two groups in two-dimensions. In the cases where the local model was a reasonable match for the nonlocal, lower values of η , we observed the local model terminated much faster given the same starting data. So, with the trials we ran, the local model saved computation time irrespective of whether the starting data was random or segregated. However, we still observe that the local approximation did not match the nonlocal model well in every case with segregated data and returned unstable results in some cases. Figure 11 illustrates a reasonable match between the minimizers of the nonlocal model and its fourth-order approximation. Note that the local minimizers are more concentrated than their

local approximations.

5. Discussion

Mechanistic models, based on local dynamics, have been used successfully to understand the leading factors in the formation of territories in different species. However, many species take nonlocal information into account and thus nonlocal mechanistic models are more suitable in those situations. Using a more realistic model comes at a computational cost and when using these models to understand population dynamics by incorporating location data of species of a group, we must solve the model numerous times as we move through a (potentially very large) parameter space. If we take into account that we might have a large system to solve (maybe double a digit number of groups), it becomes imperative that we solve the system efficiently. In this work, we explore using the energy to find minimizers and derive local approximations to determine if it is suitable to use such approximations. The main takeaway of this work is that the situation is more complex than we would like. In some cases the local approximations do a reasonable job approximating the equilibrium solutions of the nonlocal model and can be computed more efficiently; but, this was not always the case. Thus, if this method is to be used, our recommendation, is that the actual data be taken into account to help ensure that the local approximation and the nonlocal models actually match.

Acknowledgments: The authors would like to thank Mark Lewis for his helpful discussions. Both authors were partially funded by the NSF DMS-1516778.

References

- [1] A. W. Bateman, M. A. Lewis, G. Gall et al., Territoriality and home-range dynamics in meerkats, Suricata suricatta: A mechanistic modelling approach, Journal of Animal Ecology, 2015, 84(1), 260–271.
- [2] J. Bedrossian, N. Rodríguez and A. Bertozzi, Local and global well-posedness for aggregation equations and Patlak-Keller-Segel models with degenerate diffusion, Nonlinearity, 2011, 24(6), 1–31.
- [3] A. Bernoff and C. Topaz, Biological aggregation driven by social and environmental factors: A nonlocal model and its degenerate cahn-hilliard approximation, SIAM Journal on Applied Dynamical Systems, 2015, 15(3), 1528–1562.
- [4] A. Bertozzi and D. Slepcev, Existence and uniqueness of solutions to an aggregation equation with degenerate diffusion, Communications on Pure and Applied Analysis, 2010, 9(6), 1617–1637.
- [5] N. S. Clayton, P. D. Griffiths, N. J. Emery and A. Dickinson, *Elements of episodic-like memory in animals.*, Philosophical Transactions of the Royal Society of London Series B, Biological Sciences, 2001, 356(1972), 1483–1491.
- [6] J. Clobert, E. Danchin, A. Dhondt and J. D. Nichols, *Dispersal*, Oxford University Press, Oxford, 2001.
- [7] M. Heideman, D. Johnson and C. Burrus, Gauss and the history of the fast fourier transform, Archive for History of Exact Sciences, 1985, 34, 265–277.
- [8] D. Li and X. Zhang, On a nonlocal aggregation model with nonlinear diffusion, Discrete and Continuous Dynamical Systems, 2010, 27(1), 301–323.

- [9] P. K. Molnár, A. E. Derocher, T. Klanjscek and M. A. Lewis, *Predicting climate change impacts on polar bear litter size.*, Nature communications, 2011, 2, 186.
- [10] P. Moorcoft, M. A. Lewis and R. Crabree, *Home range analysis using a mechanistic home range model*, Ecology, 1999, 80(5), 1656–1665.
- [11] K. Oelschläger, A law of large numbers for moderately interacting diffusion processes, Z. Wahrscheinlichkeitstheorie verw. Gebiete, 1985, 69, 279–322.
- [12] K. Oelschläger, Large Systems of Interacting Particles and the Porous Medium Equation, Journal of Differential Equations, 1990, 88, 294–346.
- [13] C. Parmesan and G. Yohe, A globally coherent fingerprint of climate change impacts across natural systems, Nature, 2003, 421(6918), 37–42.
- [14] J. R. Potts and M. A. Lewis, Spatial Memory and Taxis-Driven Pattern Formation in Model Ecosystems, Bulletin of Mathematical Biology, 2019, 81(7), 2725–2747.
- [15] N. Rodríguez and L. Ryzhik, Exploring the effects of social preference, economic disparity, and heterogeneous environments on segregation, Communications in Mathematical Sciences, 2016, 14(2), 363–387.
- [16] N. Rodríguez and Y. Hu, On the steady-states of a two-species non-local cross-diffusion model, Journal of Applied Analysis, 2020, 26(1), 1–19.
- [17] O. Ronce, How Does It Feel to Be Like a Rolling Stone? Ten Questions About Dispersal Evolution, Annual Review of Ecology, Evolution, and Systematics, 2007, 28, 231–253.
- [18] E. J. Routh, A Treatise on the Stability of a Given State of Motion, Particularly Steady Motion, London: Macmillan and Co, 1877.
- [19] N. C. Stenseth, A. Mysterud, G. Ottersen et al., *Ecological effects of climate fluctuations*, Ecology and climatology, 2002, 297, 1292–1296.
- [20] L. Wasserstein, Markov processes over denumerable products of spaces describing large systems of automata., Problems of Information Transmission, 1969, 5, 47–52.
- [21] K. White, M. Lewis and J. Murray, A model for wolf-pack territory formation and maintenance, Journal of Theoretical Biology, 1996, 178, 29–43.
- [22] K. A. J. White, J. D. Murray and M. A. Lewis, Wolf-Deer Interactions: A Mathematical Model, Proceedings of the Royal Society B: Biological Sciences, 1996, 263(1368), 299–305.
- [23] S. Zaytseva, J. Shi and L. B. Shaw, Model of pattern formation in marsh ecosystems with nonlocal interactions, Journal of Mathematical Biology, 2020, 80, 655–686.